Performance of the Cross-Correlator Receiver for Binary Digital Frequency Modulation

Kevin A. Farrell, *Member, IEEE*, and Peter J. McLane, *Fellow, IEEE*

***Abstract*— The error probability of the cross-correlator receiver for binary digital frequency modulation (FM) detection is studied using theoretical analysis and computer simulations. The index of performance is taken as the bit-error rate (BER). The BER results obtained permit the selection of an optimum combination of modulation index and receiver bandwidth. This selection is carried out and is compared for analysis based on both computer simulation and theoretical calculation. The performance of the cross correlator is also compared to that of the limiter–discriminator, and is found to be similar. This is noteworthy because the general I/Q demodulator structure of the cross correlator is ideally suited to DSP chip implementation, and furthermore, severe amplitude limiting does not have to be performed on the input signal to the receiver. Input signal amplitude variations of up to 20% of the average signal value can be tolerated with only a 1-dB loss in performance, and the receiver is completely independent of the rate of amplitude variation. The theoretical analysis of the receiver uses a Fourier series approach [1] which takes into account the effects of FM distortion and intersymbol interference (ISI). Theoretical and simulation results are found to agree within 0.5 dB in E_b/N_o. We also address the issue of timing recovery. Results obtained indicate that losses due to timing error can be reduced to less than 0.5 dB in E_b/N_o.**

***Index Terms*— PAmplitude variation, asynchronous timing recovery, cross-correlator receiver, digital frequency modulation, Fourier analysis, *I–Q* receiver, limiter–discriminator receiver, modified Bessel function of third kind, modulation index, 30-bit "n" signal.**

I. Introduction

THE cross-correlator receiver was first proposed by Park [2] who studied the wide-band analog case. Park determined that at low signal-to-noise ratios (SNR), the performance of the cross correlator is superior to that of the limiter–discriminator. The performance of the limiter–discriminator degrades badly at low SNR due to the presence of "click noise" in the receiver. The cross correlator does not suffer from this effect because amplitude limiting is not performed to remove amplitude fluctuations. Based on his results, Park further concluded that the cross correlator could be especially useful in the detection of frequency-shift keying (FSK) in telemetry systems. Other authors have examined the cross-correlator structure, but from a somewhat different perspective. Cahn [3], Gardner [4], and Natali [5] have all studied the cross correlator as a frequency-difference detector for frequency tracking. In addition, the receiver under study has an I-Q structure and, accordingly, with firmware changes on a DSP chip can be used to demodulate either FSK, phase-shift keying (PSK), or QAM modulations.

In this study, we analyze the cross correlator for binary, continuous-phase FSK (CPFSK) detection using both Monte Carlo computer simulations and theoretical analysis. The results obtained allow a performance comparison with other conventional noncoherent CPFSK receivers. The approach used for the theoretical analysis is similar to that employed by Tjhung and Wittke [1] to study the limiter–discriminator receiver. The analysis uses a Fourier series approach which takes into account the effects of frequency modulation (FM) distortion and ISI. Theoretical and simulation results are compared, and are found to be in good agreement.

The issue of timing recovery is addressed using a timing recovery algorithm suggested by Gardner [6]. Koblents [7] studied Gardner's algorithm for PSK systems, and found that using this method of timing recovery bit-error rate (BER) performance close to theoretical maximums on the additive white Gaussian noise (AWGN) channel can be achieved. We find similar results for CPFSK detection using the cross-correlator receiver structure.

An outline of the paper is as follows. Section II contains a performance analysis via a digital computer simulation. In Section III, a mathematical analysis is presented to provide a basis for the simulation results. Section IV presents the performance of a system for timing recovery, and section V contains the conclusions.

II. Description and Simulation of the Cross-Correlator Receiver

A. Operating Principle

The system under study is the cross correlator receiver structure shown in Fig. 1. To gain insight into the operation of the receiver, consider the case where the receiver input is a single sinusoid of the form

$$s(t) = A\cos(\omega_i t + \theta_i) \tag{1}$$

where ω_i is one of two possible values corresponding to a binary 1 or 0 and θ_i is the constant phase offset of the signal. The received signal is mixed to baseband, and low-pass filtered to remove double-frequency terms yielding the outputs

$$I = A\cos(\Delta\omega t + \theta) \tag{2}$$

$$Q = -A\sin(\Delta\omega t + \theta) \tag{3}$$

Paper approved by M. J. Joindot, the Editor for Radio Communications of the IEEE Communications Society. Manuscript received January 8, 1995; revised December 1, 1995 and October 1, 1996. This work was supported by the Telecommunications Research Institute of Ontario (TRIO). Results from this paper were presented at Wireless'94 and at IEEE Globecom'94.

The authors are with the Department of Electrical & Computer Engineering, Queen's University, Kingston, Ont., K7L 3N6 Canada.

Publisher Item Identifier S 0090-6778(97)03716-1.

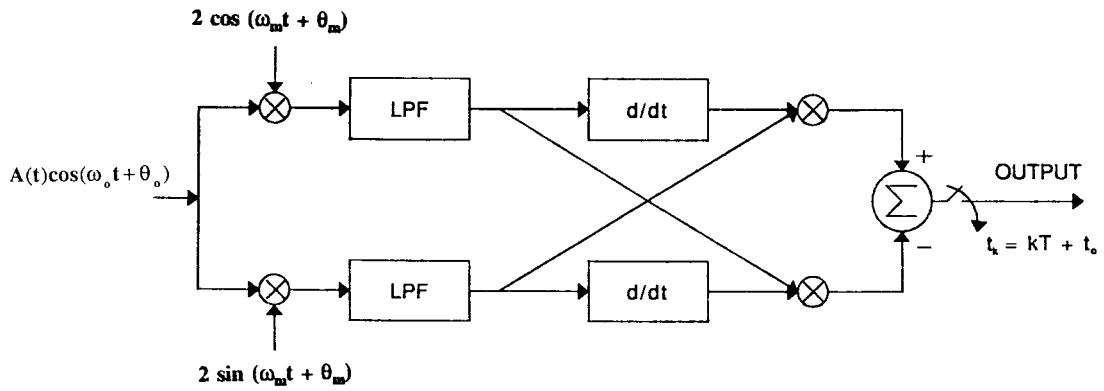

Fig. 1. Cross-correlator receiver.

where $\Delta\omega = \omega_1 - \omega_m, \theta = \theta_i - \theta_m, \omega_m$ is the radian mixing frequency, and θ_m is the initial phase offset of the mixing signal. Differentiation of the filtered output on both the in-phase and quadrature rails gives

$$\dot{I} = -A\Delta\omega \sin(\Delta\omega t + \theta) \tag{4}$$

$$\dot{Q} = -A\Delta\omega \cos(\Delta\omega t + \theta) \tag{5}$$

where a dot over a variable denotes differentiation with respect to time. The output of the cross-correlator receiver in Fig. 1, V_o, is

$$\begin{aligned} V_o &= \dot{I}Q - \dot{Q}I \\ &= A^2\Delta\omega \sin^2(\Delta\omega t + \theta) + A^2\Delta\omega \cos^2(\Delta\omega t + \theta) \\ &= A^2\Delta\omega. \end{aligned} \tag{6}$$

That is, the output of the cross correlator is proportional to the frequency difference between the transmitted frequency and the mixing frequency. Notice that neither the initial phase of the transmitted signal nor that of the mixing signal has any effect on the receiver output.

If we assume that the probability of transmitting a 1 is equal to the probability of transmitting a 0, then, given the symmetry of the receiver, the probability of error is minimized for any arbitrary E_b/N_o when the mixing frequency is equal to the carrier frequency of the transmitted signal. This means that if a 1 is sent, the output of the receiver is $+\omega_d$ and $-\omega_d$ if a 0 is sent, where ω_d is the radian frequency deviation. Further, the decision threshold for the receiver bit detector should be set at zero.

B. Simulation Model

In our simulation model, a CPFSK signal corrupted with AWGN is input to the receiver. The low-pass filters in the receiver serve a dual purpose. The obvious function of the filters is to remove the double-frequency terms produced by mixing in the receiver's front end of Fig. 1. However, they are also responsible for reducing the noise power in the receiver, which requires a narrow filter bandwidth. Conflicting with this requirement is the fact that to pass an undistorted signal to the detector, a wide filter bandwidth is required. There exists an optimum solution to this problem. Tjhung and Wittke [1] determined that for FSK systems in a restricted band, a bandwidth of about 1.2 times the symbol rate (i.e., a BT product of 1.2) in the case of a filter with sharp cutoff and about 1.0 for a filter with a more gradual rolloff, combined with a peak-to-peak frequency deviation of about 0.7 times the bit rate, yields a minimum probability of error. The precise value of the optimum BT product depends upon the shape of the particular filter and the value of the input E_b/N_o. All LPF's used in our simulations are Kaiser windowed, approximate ideal low-pass FIR filters of length 30 taps.

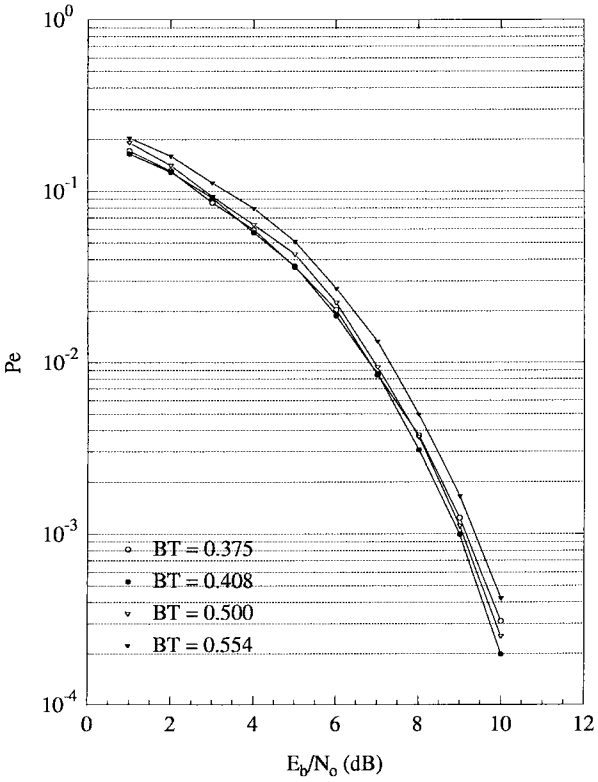

Fig. 2. Error rate for binary CPFSK as a function of E_b/N_o $h = 0.67$.

The differentiators in the simulation are modeled using a first-order finite-difference approximation. We used eight samples per symbol in all simulations. The first-order difference approximation worked well using eight samples per symbol. More accurate approximations are possible, but at the cost of increased system complexity.

C. Cross-Correlator Performance

The simulation result for the BER for the cross correlator is shown in Fig. 2 for a modulation index of 0.67 and normalized

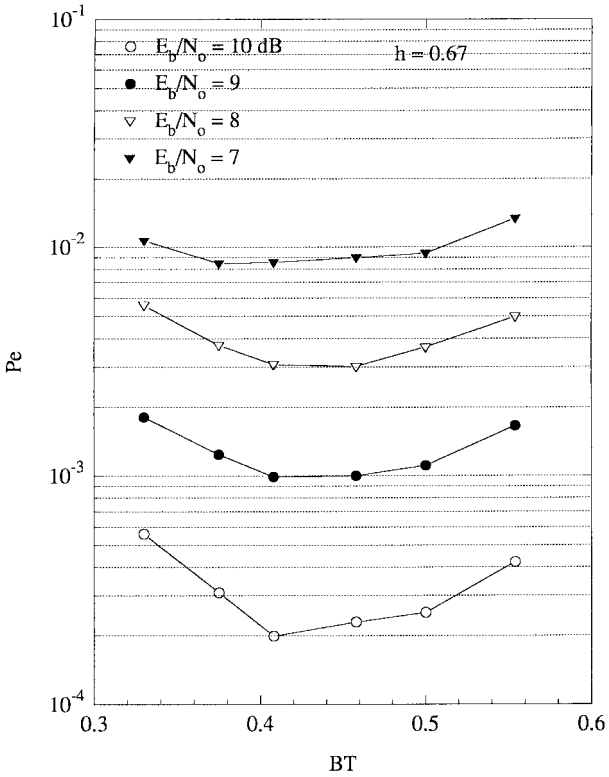

Fig. 3. Error rate for binary CPFSK as a function of filter bandwidth $h = 0.67$.

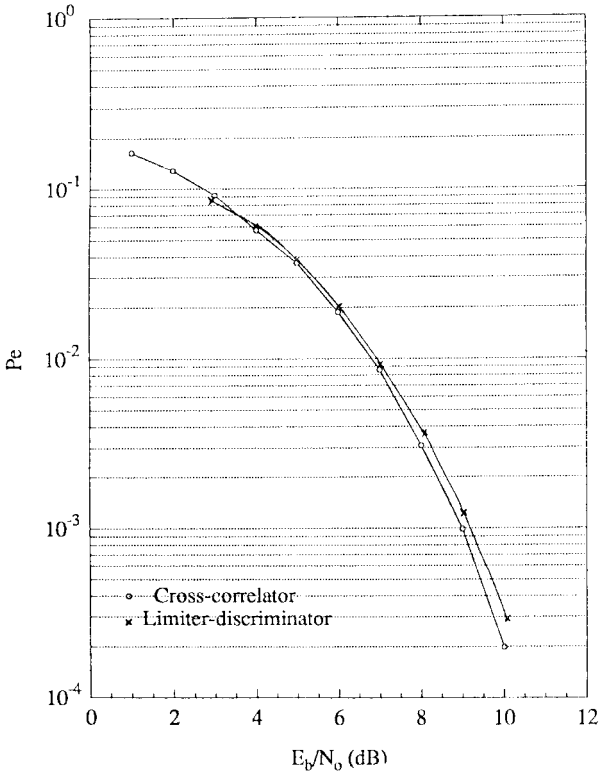

Fig. 4. Comparison of cross correlator and limiter–discriminator performance.

bandwidth. All modulation indexes that we consider are less than 1, corresponding to narrow-band FM. A modulation index h equal to 0.67 consistently gives the lowest BER for all values of BT and E_b/N_o. The increase in the BER as h is increased is a consequence of the spectrum broadening for large values of h, leading to more distortion of the low-pass filtered signal. As h decreases, the output signal of the filter becomes small and, therefore, difficult to detect in the presence of noise at the receiver output. The above arguments suggest that there is an optimum value of h. The simulation results that we have obtained indicate that this value is around 0.67. Many other results of this nature, including the effect of pulse shaping, can be found in [12].

Another way of examining the results is to plot the BER curves as a function of the BT product. Fig. 3 presents a typical result for the best modulation index of 0.67 for various values of E_b/N_o. Note that for each modulation index, there exists a bandwidth which minimizes the probability of error, and that best performance is not sensitive to perturbations from the optimum receiver bandwidth. As the bandwidth of the system is increased, both the noise and signal energy entering the receiver increase. However, there is an optimum system bandwidth corresponding to the best tradeoff between signal distortion and noise attenuation. The best performance of the cross correlator is obtained for a BT product and modulation index combination of $h = 0.67$ and $BT = 0.408$.

D. Comparison with the Limiter–Discriminator

Park [2] concluded that the performance of the cross correlator is superior to that of the classical limiter–discriminator for the wide-band analog FM case at low SNR. We now compare the performance of the cross correlator to that of the limiter–discriminator for binary CPFSK detection.

In Fig. 4, the BER performance of the cross correlator and the limiter–discriminator are compared for the best modulation index and filter bandwidth found earlier. The results shown for the limiter–discriminator were presented by Tjhung and Wittke [1]. Before continuing, it should be pointed out that the filter used to produce the results for the limiter–discriminator is a Gaussian filter, while that used for the cross correlator structure is based on Kaiser windowing of the unit sample response of an ideal low-pass filter. Reference to Fig. 4 indicates that the performance of the cross correlator is slightly superior to that of the limiter–discriminator. The improvement in performance is small and, therefore, cannot be considered significant in practice.

E. Effect of Time-Varying Input Signal Amplitude

Thus far, we have assumed that the input to the receiver is a constant amplitude signal. In practice, amplitude fluctuations are present in the input signal as a result of nonideal channel conditions and amplifier nonlinearities. We now investigate the effect of the receiver performance when amplitude variations are introduced into the input signal.

Consider the case where the receiver input is a sinusoid of the form

$$s(t) = A(t)\cos(\omega_i t + \theta_i) \tag{7}$$

where $A(t)$ is a slow time-varying amplitude. The received signal is mixed to baseband and low-pass filtered to remove

the double-frequency terms produced, yielding

$$I = A(t)\cos(\Delta\omega t + \theta) \tag{8}$$

$$Q = -A(t)\sin(\Delta\omega t + \theta) \tag{9}$$

where $\Delta\omega = \omega_1 - \omega_m, \theta = \theta_i - \theta_m, \omega_m$ is the radian mixing frequency, and θ_m is the initial phase offset of the mixing signal. Differentiation of the filtered output on both the in-phase and quadrature rails gives

$$\dot{I} = \dot{A}(t)\cos(\Delta\omega t + \theta) - A(t)\Delta\omega\sin(\Delta\omega t + \theta) \tag{10}$$

$$\dot{Q} = \dot{A}(t)\sin(\Delta\omega t + \theta) - A(t)\Delta\omega\cos(\Delta\omega t + \theta) \tag{11}$$

where, as before, a dot over a function denotes differentiation with respect to time. The output of the receiver V_o is given as

$$V_o = \dot{I}Q - \dot{Q}I = A^2(t)\Delta\omega. \tag{12}$$

The output of the receiver is proportional to both the frequency difference between the transmitted frequency and the mixing frequency and the amplitude squared of the input signal. Notice that all terms containing the variable $\dot{A}(t)$ cancel out, and do not appear in the final expression. Therefore, varying the input amplitude causes the magnitude of the output signal to change, but has no effect on the sign of the output.

In our simulation model, we introduced a sinusoidal amplitude variation of the form

$$A(t) = A[1 + \mu\cos(\omega_A t)] \tag{13}$$

where μ is the amplitude modulation index of the sinusoidal amplitude variation and ω_A is the radian frequency of the signal envelope. The envelope frequency chosen corresponds to an envelope period of 500 symbols. Performance results for the receiver with the sinusoidal time-varying signal amplitude are shown in Fig. 5 for $\mu = 0.1$ and 0.2. Notice that the BER is plotted as a function of average E_b/N_o. For the case of $\mu = 0.1$, there is approximately a 0.25-dB degradation in performance compared to a 1-dB degradation for the case where $\mu = 0.2$. The reason for this degradation is that, as the signal amplitude decreases below its average value, the probability of bit error increases.

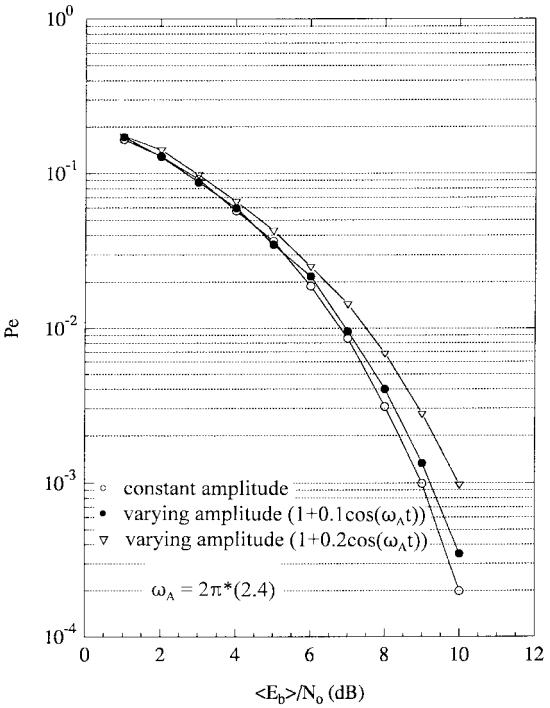

Fig. 5. Performance of the cross correlator with a time-varying input signal amplitude.

III. Theoretical Analysis

A. Analysis by a Fourier Method

In this section, we present the theoretical performance analysis of the cross correlator receiver for binary CPFSK detection in the presence of AWGN. While this analysis is fairly accurate, some reasonable assumptions are made in the interest of tractability.

The CPFSK signal can be written as

$$s(t) = \mathrm{Re}\{A\exp j[\omega_c t + m(t)]\} \tag{14}$$

where A is the carrier amplitude, ω_c is the radian carrier frequency, and the message signal is

$$m(t) = \omega_d \int_{-\infty}^{t} b(\tau)\,d\tau + \theta_i. \tag{15}$$

The function $b(t)$ is the baseband signal that modulates the carrier frequency, and θ_i is the initial phase of the signal. Ideally, $b(t)$ should be modeled as a random, binary signal and zero mean. However, due to the presence of ISI, a pseudorandom sequence will be used here as the modulating baseband signal to make the analysis tractable. The technique of using pseudorandom sequences has been used previously by other authors. Tjhung and Wittke [1] used it to evaluate the performance of the limiter–discriminator. In this analysis, we use the same 30-bit "n" signal [8] employed by Tjhung and Wittke.

Since $b(t)$ is periodic and has zero mean, $\exp[jm(t)]$ is a periodic function having the same period as $b(t)$, and can be represented by the Fourier series

$$\exp[jm(t)] = \sum_{n=-\infty}^{\infty} C_n \exp(jn\omega_o t) \tag{16}$$

where the complex Fourier series coefficient is

$$C_n = \frac{1}{T_o}\int_{-(T_0/2)}^{T_o/2} \exp j(m(t) - n\omega_o t)\,dt \tag{17}$$

and $T_o = 2\pi/\omega_o$ is the period of $b(t)$. Therefore, by substitution of (16) into (14), the FM signal $s(t)$ becomes

$$s(t) = \mathrm{Re}\left\{A\sum_{n=-\infty}^{\infty} C_n \exp j(\omega_c + n\omega_o)t\right\}. \tag{18}$$

Mixing to baseband and low-pass filtering produces the in-phase and quadrature components

$$I(t) = \mathrm{Re}\left\{A\sum_{n=-\infty}^{\infty} C_n H(n\omega_o)\exp j(n\omega_o t)\right\} \tag{19}$$

$$Q(t) = -\mathrm{Im}\left\{A \sum_{n=-\infty}^{\infty} C_n H(n\omega_o) \exp j(n\omega_o t)\right\} \quad (20)$$

where $H(\omega)$ is the transfer function of the receiver filters. Note that it is assumed that the sum frequency components produced by mixing are completely suppressed by the low-pass filters.

Define a rectangular filter as an idealized filter with a flat transmission characteristic in the passband and zero transmission in the stopband. This is the filter that we approximated with the windowed, FIR filter used in the simulations. Incorporating the rectangular filter model into the analysis, (19) and (20) become

$$I(t) = \mathrm{Re}\left\{A \sum_{n=-M}^{M} C_n \exp j(n\omega_o t)\right\} \quad (21)$$

$$Q(t) = -\mathrm{Im}\left\{A \sum_{n=-M}^{M} C_n \exp j(n\omega_o t)\right\} \quad (22)$$

where M is the number of harmonics contained in the filter passband of width B Hz.

The complex coefficient in (17), C_n, can be represented in its real and imaginary parts as

$$C_n = C_{1n} + jC_{2n}. \quad (23)$$

Substituting (23) into (21) and (22) gives

$$I(t) = \mathrm{Re}\left\{A \sum_{n=M}^{M} [C_{1n} + jC_{2n}] \exp\ j(n\omega_o t)\right\} \quad (24)$$

$$Q(t) = -\mathrm{Im}\left\{A \sum_{n=-M}^{M} [C_{1n} + jC_{2n}] \exp j(n\omega_o t)\right\}. \quad (25)$$

We now simplify (24) and (25) by finding the real and imaginary parts as indicated to produce

$$I(t) = A \sum_{n=-M}^{M} [C_{1n} \cos(n\omega_o t) - C_{2n} \sin(n\omega_o t)] \quad (26)$$

$$Q(t) = -A \sum_{n=-M}^{M} [C_{1n} \sin(n\omega_o t) + C_{2n} \cos(n\omega_o t)]. \quad (27)$$

Equations (26) and (27) can be written in polar form as

$$I(t) = A \sum_{n=-M}^{M} |C_n| \cos(n\omega_o t + \theta_n) \quad (28)$$

$$Q(t) = -A \sum_{n=-M}^{M} |C_n| \sin(n\omega_o t + \theta_n) \quad (29)$$

where

$$|C_n|^2 = C_{1n}^2 + C_{2n}^2 \quad (30)$$

and

$$\theta_n = \tan^{-1}\left(\frac{C_{2n}}{C_{1n}}\right). \quad (31)$$

Differentiating $I(t)$ and $Q(t)$ in (28) and (29), respectively, with respect to time gives

$$\dot{I}(t) = -A \sum_{n=-M}^{M} n\omega_o |C_n| \sin(n\omega_o t + \theta_n) \quad (32)$$

$$\dot{Q}(t) = -A \sum_{n=-M}^{M} n\omega_o |C_n| \cos(n\omega_o t + \theta_n). \quad (33)$$

The output of the receiver $V_o(t)$ in (12) is given by

$$\begin{aligned} V_o(t) &= \dot{I}Q - \dot{Q}I \\ &= \left[A \sum_{n=-M}^{M} |C_n| \cos(n\omega_o t + \theta_n)\right] \\ &\quad \cdot \left[A \sum_{n=-M}^{M} n\omega_o |C_n| \cos(n\omega_o t + \theta_n)\right] \\ &\quad + \left[A \sum_{n=-M}^{M} |C_n| \sin(n\omega_o t + \theta_n)\right] \\ &\quad \cdot \left[A \sum_{n=-M}^{M} n\omega_o |C_n| \sin(n\omega_o t + \theta_n)\right]. \end{aligned} \quad (34)$$

The output of the receiver corresponding to (34) was reconstructed for various bandwidths with the aid of a computer. Fig. 6(a) and (b) represents plots of the receiver output as a function of time for four different bandwidths. The receiver output is normalized to the radian frequency deviation and time is normalized to the symbol period. Notice that, as the receiver bandwidth is reduced, the effects of ISI and FM distortion become very apparent.

B. CPFSK Analysis in the Presence of AWGN

In the previous section, the output of the receiver due to a CPFSK signal was determined, and is given in (34). We now extend that analysis to include noise. The expression for the CPFSK signal in (14) corrupted by AWGN can be represented as

$$r(t) = \mathrm{Re}\{A \exp j[\omega_c t + m(t)]\} + n(t) \quad (35)$$

where $m(t)$ is given in (15) and $n(t)$ is Gaussian noise having a two-sided spectral density of $N_o/2$ W/Hz. Once again the function $b(t)$ will be modeled as a periodic, pseudorandom sequence. The Gaussian noise process $n(t)$ can be represented in terms of in-phase and quadrature components as

$$n(t) = n_1(t) \cos(\omega_c t) + n_2(t) \sin(\omega_c t) \quad (36)$$

where $n_1(t)$ and $n_2(t)$ are independent Gaussian random processes each having a two-sided spectral density of N_o W/Hz. Therefore, with reference to (35), the received signal $r(t)$ can be rewritten as

$$\begin{aligned} r(t) = \mathrm{Re}&\left\{A \sum_{n=-\infty}^{\infty} C_n \exp j(\omega_c + n\omega_o)t\right\} \\ &+ n_1(t) \cos(\omega_c t) + n_2(t) \sin(\omega_c t). \end{aligned} \quad (37)$$

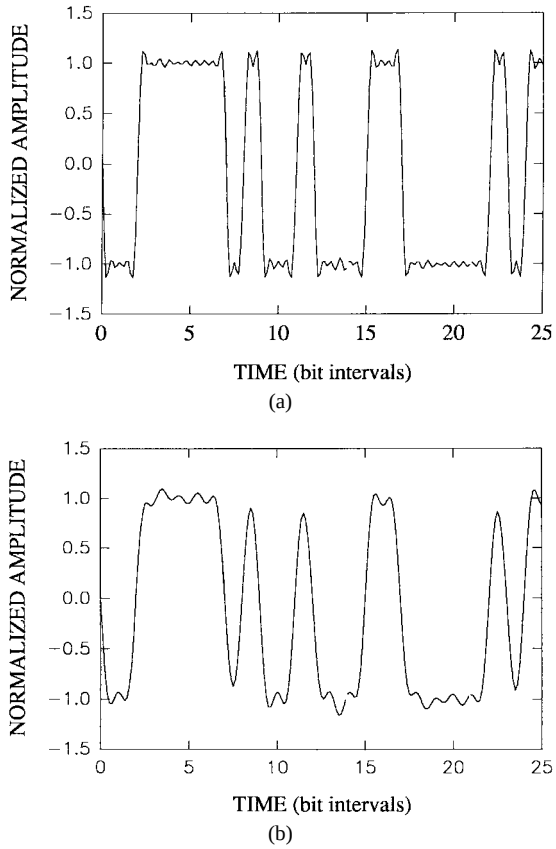

Fig. 6. (a) Theoretical output of the cross correlator. $h = 0.67$, $BT = 1.67$. (b) Theoretical output of the cross correlator. $h = 0.67$, $BT = 0.6$.

The analysis to obtain an expression for the receiver output due to the noise corrupted input signal represented by (37) is very similar to the analysis presented in the previous section, and therefore only the result will be given. The voltage $V_o(t)$ in (12) will be decomposed into signal and noise terms. The signal term is given in (34). The noise term is derived below. A complete derivation can be found in [12].

The expression for the noise output of the receiver $V_{\text{NOISE}}(t)$ is

$$\begin{aligned} V_{\text{NOISE}}(t) = {} & n_1 A \sum_{n=-M}^{M} n\omega_o |C_n| \cos(n\omega_o t) \\ & - n_2 A \sum_{n=-M}^{M} n\omega_o |C_n| \sin(n\omega_o t) \\ & - \dot{n}_1 A \sum_{n=-M}^{M} |C_n| \sin(n\omega_o t) \\ & - \dot{n}_2 A \sum_{n=-M}^{M} |C_n| \cos(n\omega_o t) \\ & + \dot{n}_1 n_2 - n_1 \dot{n}_2 \end{aligned} \tag{38}$$

where M is the number of harmonics contained in the filter passband of width B Hz. The first two terms of (38) can be added to form a Gaussian random process with variance

$$\sigma_1^2 = \sigma_n^2 A^2 \sum_{n=-M}^{M} (n\omega_o)^2 |C_n|^2 \tag{39}$$

where σ_n^2 is defined to be the variance of the Gaussian processes n_1 and n_2, bandlimited to B Hz. Similarly, the third and fourth terms of (38) can also be summed to yield another Gaussian random variable with variance

$$\sigma_2^2 = \sigma_{\dot{n}}^2 A^2 \sum_{n=-M}^{M} |C_n|^2. \tag{40}$$

The variable C_n was defined in (17). However, C_n has other significance. $|C_n|^2$ is the power of the transmitted frequency-modulated signal contained in the nth harmonic. Thus, we can rewrite (39) and (40) as

$$\sigma_1^2 = \sigma_n^2 A^2 \int_{-2\pi B}^{2\pi B} \left[\sum_{n=-\infty}^{\infty} (n\omega_o)^2 |C_n|^2 \delta(\omega - n\omega_o) \right] d\omega \tag{41}$$

and

$$\sigma_2^2 = \sigma_n^2 A^2 \int_{-2\pi B}^{2\pi B} \left[\sum_{n=-\infty}^{\infty} |C_n|^2 \delta(\omega - n\omega_o) \right] d\omega \tag{42}$$

where B is the receiver filter bandwidth measured in hertz and $\delta(x)$ is the delta function. Note that the power spectral density (PSD) of the transmitted signal, $s(t)$ is

$$\text{PSD}(\omega) = \sum_{n=-\infty}^{\infty} |C_n|^2 \delta(\omega - n\omega_o) \tag{43}$$

Consider now the effect on (41) and (42) if the baseband signal is modeled as a random binary signal rather than as a periodic pseudorandom signal as has been considered up to this point. Denote the spectral density function of this random bit input CPFSK signal as $\Phi(\omega)$. $\Phi(\omega)$ is a continuous function of ω. Therefore, if the input bit sequence is modeled as a random binary sequence, the corresponding expressions for (41) and (42) are

$$\sigma_1^2 = \sigma_n^2 A^2 \int_{-2\pi B}^{2\pi B} \omega^2 \Phi(\omega)\, d\omega \tag{44}$$

and

$$\sigma_2^2 = \sigma_{\dot{n}}^2 A^2 \int_{-2\pi B}^{2\pi B} \Phi(\omega)\, d\omega. \tag{45}$$

A generalized expression for the power spectral density of M-ary CPFSK is given by Proakis [9, p. 200]. Therefore, we can evaluate (44) and (45) using results from [9]. In further analysis to follow, (44) and (45) will be used rather than (39) and (40) because they are exact expressions and not approximations.

Thus far, we have not considered the final two terms of (38), $\dot{n}_1 n_2$ and $n_1 \dot{n}_2$. These terms are non-Gaussian. The probability density function (pdf) of these two non-Gaussian terms is derived in [12]. This result will be used to determine the pdf of the cross correlator noise output.

C. Probability Density Function (pdf) of the Cross-Correlator Noise Output

We now determine the pdf of the noise at the receiver output as given in (38). The cross correlation of n_1 and $\dot{n}_1, R_{n_1\dot{n}_1}(\tau)$, is given as

$$R_{n_1\dot{n}_1}(\tau) = \frac{j}{2\pi}\int_{-\infty}^{\infty} \omega S_{n_1 n_1}(\omega) e^{j\omega\tau}\, d\tau \tag{46}$$

where $S_{n_1 n_1}(\tau)$ is the spectral density of n_1. It follows from (46) that $R_{n_1\dot{n}_1}(0) = 0$ since $S_{n_1,n_1}(\omega)$ is an even function of ω. Therefore, at any instant of time, n_1 and $\dot{n}_1$ are uncorrelated. Further, since n_1 and $\dot{n}_1$ are Gaussian, it follows that they are also independent. Similarly, n_2 and $\dot{n}_2$ are also independent, and thus it follows that all noise terms in (38) are independent.

Recall the expression for the noise output of the receiver given by (38) and rewritten below in the general form

$$\begin{aligned} V_{\text{NOISE}} = {} & p\dot{q} - q\dot{p} + (Ap + B\dot{q})\cos(\omega t) \\ & + (Aq - B\dot{p})\sin(\omega t) \end{aligned} \tag{47}$$

where A and B are constants. Here, p, q, and the sum of the final two terms of (47) are Gaussian random variables with zero mean. Note that both p and q have the same variance σ_p^2. Similarly, $\dot{p}$ and $\dot{q}$ also have the same variance $\sigma_{\dot{q}}^2$. The terms $p\dot{q}$ and $q\dot{p}$ are not Gaussian, but each has mean zero and pdf $f_z(z)$ given in [12]. Written in terms of p and q, we have for $z = p\dot{q}$

$$f_z(z) = \frac{1}{\pi\sigma_p\sigma_{\dot{q}}} K_o\left(\frac{|z|}{\sigma_p\sigma_{\dot{q}}}\right) \tag{48}$$

where $K_o(x)$ is the modified Bessel function of the third kind [11]. The result for $z = q\dot{p}$ is determined by interchanging the subscripts p and $\dot{q}$ in (48), and thus has the same pdf.

It is necessary to determine the pdf of V_{NOISE} in (47). Define a new variable x as

$$x = (Ap + B\dot{q})\cos(\omega t) + (Aq - B\dot{p})\sin(\omega t). \tag{49}$$

That is, x represents the Gaussian components of the receiver noise output. We proceed by multiplying the Fourier transforms of $p\dot{q}, q\dot{p}$, and x. The Fourier transform of $x, F_x(y)$, referred to as the characteristic function or moment generating function, is given by [10] as

$$F_x(y) = F\left\{\frac{1}{\sigma_x\sqrt{2\pi}} e^{-x^2/2\sigma_x^2}\right\} = e^{-\sigma_x^2 y^2/2} \tag{50}$$

where σ_x^2 is the variance of x and is the sum of σ_1^2 and σ_2^2 as given by (44) and (45). Similarly, the characteristic function of either of the terms $p\dot{q}$ or $q\dot{p}, F_z(y)$, is found by taking the Fourier transform of (48), yielding [9]

$$\begin{aligned} F_z(y) &= F\left\{\frac{1}{\pi\sigma_p\sigma_{\dot{q}}} K_o\left(\frac{|z|}{\sigma_p\sigma_{\dot{q}}}\right)\right\} \\ &= \frac{1}{\sigma_p\sigma_{\dot{q}}}\left[\frac{1}{\left(\frac{1}{\sigma_p\sigma_{\dot{q}}}\right)^2 + y^2}\right]^{1/2}. \end{aligned} \tag{51}$$

We now write the Fourier transform for V_{NOISE} in (47) as $F_v(y) = F_x(y)F_z(y)F_z(y)$ to give

$$F_v(y) = \frac{1}{\sigma_p^2\sigma_{\dot{q}}^2}\left[\frac{1}{\left(\frac{1}{\sigma_p\sigma_{\dot{q}}}\right) + y^2}\right] e^{-\sigma_x^2 y^2/2}. \tag{52}$$

The density of $V_{\text{NOISE}}, f_v(v)$, is obtained by taking the inverse Fourier transform of $F_v(y)$ in (52) to yield

$$\begin{aligned} f_v(v) = {} & \frac{1}{2\sigma_p\sigma_{\dot{q}}} \exp\left(\frac{\sigma_x^2}{2\sigma_p^2\sigma_{\dot{q}}^2}\right)\left\{\exp\left(-\frac{v}{\sigma_p\sigma_{\dot{q}}}\right)\right. \\ & \cdot Q\left[\frac{\sigma_x}{\sigma_p\sigma_{\dot{q}}} - \frac{v}{\sigma_x}\right] + \exp\left(\frac{v}{\sigma_p\sigma_{\dot{q}}}\right) \\ & \left.\cdot Q\left[\frac{\sigma_x}{\sigma_p\sigma_{\dot{q}}} + \frac{v}{\sigma_x}\right]\right\} \end{aligned} \tag{53}$$

where

$$Q(v) = \int_v^{\infty} \frac{1}{\sqrt{2\pi}} e^{-t^2/2}\, dt. \tag{54}$$

This is the form of the probability distribution function of the output noise of the cross-correlator receiver. However, we need to relate the quantities σ_x, σ_p, and $\sigma_{\dot{q}}$ to quantities found in the original expression for the noise output of the receiver, (38). Comparison of (38) and (47) shows that

$$\begin{aligned} \sigma_p^2 &= \sigma_n^2 \\ \sigma_{\dot{q}}^2 &= \sigma_{\dot{n}}^2 = \sigma_n^2 \frac{(2B)^2\pi^2}{3} \end{aligned} \tag{55}$$

and $\sigma_x^2 = \sigma_1^2 + \sigma_2^2$ with σ_1^2 in (44) and σ_2^2 in (45).

E. Bit-Error Performance of the Cross Correlator

This section outlines the methodology for obtaining the BER for the cross correlator. BER results are given at the end of the section.

Equation (34) gave an expression for the output signal $V_o(t)$ of the receiver when the input is a CPFSK signal. Fig. 6(a) and (b) showed plots of the signal output of the cross-correlator receiver for various bandwidths as a function of time using this expression. With the aid of these results, the output sampled at the midsymbol was determined for each of the first 15 symbols. Only the first 15 symbols were considered because the sequence is antisymmetric, and repeats negatively over the next 15 symbols. The magnitude of the 15 values obtained from the output are then averaged, and the result is considered a valid approximation to the output of the receiver for the particular bandwidth.

Now, recall that the cross-correlator receiver is a symbol-by-symbol detector. That is, a symbol decision is made each symbol period. With reference to Fig. 1, at time $t_k = t_o + kT$, the receiver output is sampled, and a decision is made about the identity of I_k. I_k refers to the kth transmitted symbol, and t_o is the timing offset which is optimized to minimize the probability of error. The decision rule for the cross-correlator receiver when detecting binary CPFSK is

$$\hat{I}_k = \begin{cases} 1, & \text{if } V_k > 0 \\ 0, & \text{if } V_k \le 0 \end{cases} \tag{56}$$

where $\hat{I}_k$ is the receiver estimate of the kth transmitted bit and V_k denotes the output of the receiver at time t_k. Assuming that the probability of transmitting a 1 is equal to the probability of transmitting a 0, the probability of error of the cross correlator can be represented mathematically as

$$P(e) = \tfrac{1}{2}\,P(V_k > 0 | I_k = 0) + \tfrac{1}{2}\,P(V_k \le 0 | I_k = 1). \quad (57)$$

Further, if we assume that the pdf of the noise at the receiver output is symmetric about zero, then

$$P(V_k > 0 | I_k = 0) = P(V_k \le 0 | I_k = 1). \quad (58)$$

Using (58), we can rewrite (57) as

$$P(e) = P(V_k \le 0 | I_k = 1). \quad (59)$$

We now approximate the output of the receiver at time t_k as

$$V_k = V_{\mathrm{AVG}} + V_{\mathrm{NOISE}}(kT) \quad (60)$$

where $V_{\mathrm{NOISE}}(t)$ is given by (38) and the method of determining V_{AVG} was given previously. Therefore, using (59) and (60), we can express the probability of error of the receiver as

$$P(e) = P(V_{\mathrm{AVG}} + V_{\mathrm{NOISE}} \le 0). \quad (61)$$

The probability of error expressed in (61) can be written in terms of the pdf of V_{NOISE} as

$$P(e) = \int_{V_{\mathrm{AVG}}}^{\infty} f(v)\,dv \quad (62)$$

where $f_v(v)$ is the pdf of V_{NOISE} as given by (53).

In order to perform the integration of (62) to find the probability of bit error, we need to have a method of evaluating σ_n. Given that the probability of error will be expressed as a function of E_b/N_o, it is necessary to derive a relationship between σ_n and E_b/N_o. E_b/N_o is defined to be

$$\frac{E_b}{N_o} = \frac{A^2 T}{2N_o} \quad (63)$$

where T is the symbol period, A is the amplitude of the signal, and N_o is the noise power spectral density. Multiplying both the numerator and denominator of (63) by the filter bandwidth B gives

$$\frac{E_b}{N_o} = \frac{A^2 BT}{2BN_o} = \frac{A^2 BT}{\sigma_n^2}. \quad (64)$$

We now present numerical results for the performance of the receiver based on the foregoing analysis. Results are obtained for various values of BT with modulation indexes of 0.67 and 0.83 as a function of E_b/N_o. This permits comparison with the simulation results of Section II. Fig. 7 shows the theoretical BER results as a function of E_b/N_o. For modulation indexes of 0.67 and 0.83, the best performance is obtained for BT products of 0.467 and 0.5, respectively. The computer simulation results indicated that the best BT product values for modulation indexes of 0.67 and 0.83 were 0.408 and 0.458, respectively. Therefore, it can be seen that there is close agreement in the optimum BT products obtained by theory and computer simulation. In Fig. 8, the best simulation curve and the best theoretical curve for modulation index of 0.67 are compared. The theoretical and simulation curves agree within 0.5 dB. Other performance results can be found in [12].

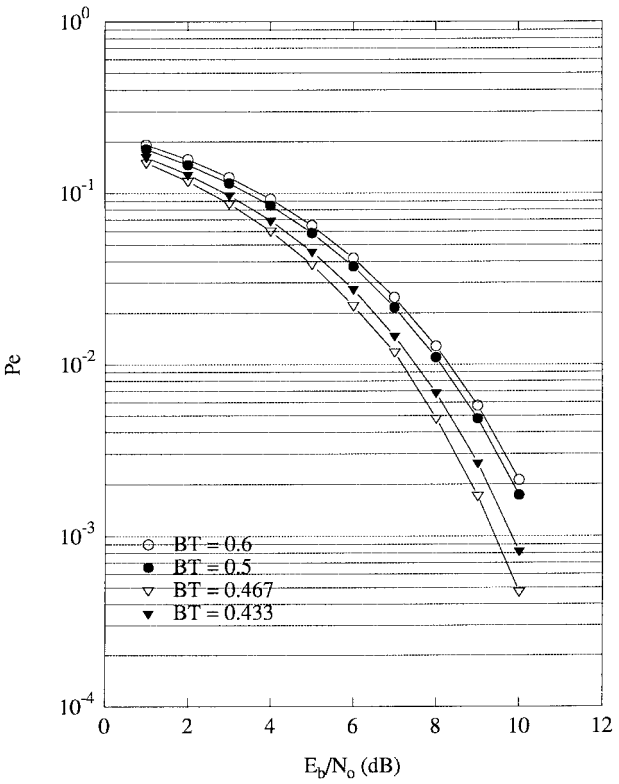

Fig. 7. Theoretical performance of the cross correlator for binary CPFSK. $h = 0.67$ and $h = 0.83$ (outer two curves).

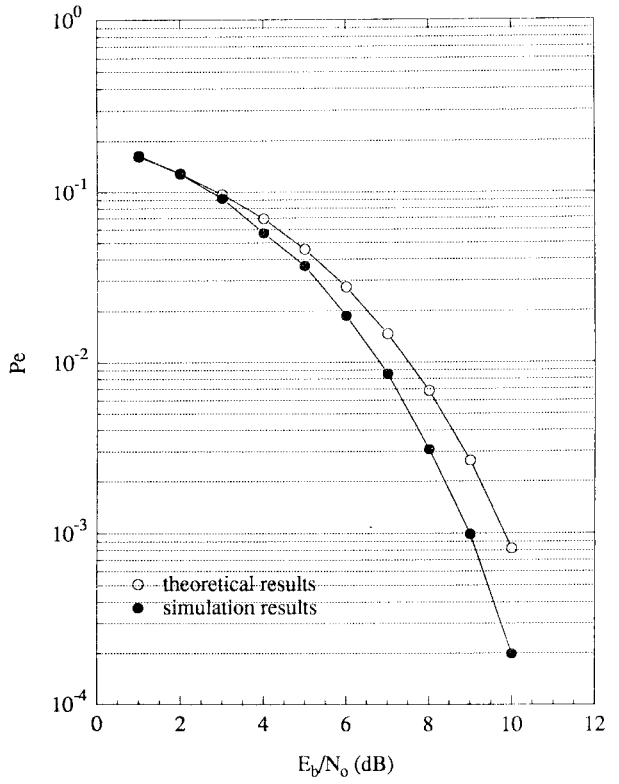

Fig. 8. Comparison of theoretical and simulation results for the cross correlator. $h = 0.67$.

IV. Timing Recovery

Up to this point, all analysis and results presented have assumed perfect timing at the receiver output. In practice, imperfect synchronization between the receiver and transmitter clocks produces timing errors at the receiver necessitating some form of timing recovery. The timing algorithm we consider in this study is essentially a zero-crossing tracker first proposed by Gardner [6]. The algorithm uses two samples per symbol and recovers timing asynchronously, that is, from the receiver samples taken from an uncontrolled A/D convertor. The fundamental equation governing the operation of the algorithm is

$$E(n) = x_{n-1/2}(x_n - x_{n-1}) \tag{65}$$

where $E(n)$ is a measure of the timing error, x_{n-1} is the receiver output for the $(n-1)$th symbol, x_n is the receiver output for the nth symbol, and $x_{n-1/2}$ is the receiver output midway in time between these symbols. If there is a data transition between the $(n-1)$th and the nth symbols, then ideally, $x_{n-1/2}$ is a zero crossing. Therefore, the deviation of $x_{n-1/2}$ from zero is related to the amount of timing error present in the system. Note that $E(n) \simeq 0$ for no symbol transition as $x_n \simeq x_{n-1}$. Also, the term $x_n - x_{n-1}$ ensures that the timing correction is in the right direction.

Koblents [7] found that initial implementations of the timing algorithm resulted in much poorer performance than anticipated. It was noted that residual error terms produced by detection of a genuine timing error caused the detector to constantly correct for false errors, producing excess timing jitter. The problem was solved by employing a loop filter and error threshold. Like Koblents, we use a first-order IIR filter as our loop filter described by the first-order difference equation

$$y(k) = BE(k) + A[y(k-1)]. \tag{66}$$

In our simulations, we chose $A = 0.875$ and $B = 0.125$, and the timing drift was set at 1 sample/50 symbols. Note that the loop filter serves a dual purpose. In addition to reducing the influence of the residual timing error, it also reduces the noise entering the detector. Timing corrections are made when the absolute value of the error signal exceeds a threshold level. Using our simulation model, we determined the error signal value corresponding to a one sample timing offset. The threshold value was set to 70% of this value.

In Fig. 9, we compare the performance of the cross correlator with timing drift present versus the receiver performance with perfect timing at the receiver output. The results indicate that using Gardner's timing algorithm, losses due to timing error can be reduced to about 0.5 dB in E_b/N_o. The timing offset was set at one sample value every 50 transmitted symbols. Thus, the timing jitter has a bandwidth of one-fiftieth of the bit rate. This is actually a large bandwidth for most DSP-based modem applications.

V. Conclusions

In this study, the performance of the cross correlator receiver for binary digital CPFSK detection was determined. It was found that the BER performance of the cross correlator is similar to that of the limiter–discriminator to within 0.2 dB in E_b/N_o. Results obtained indicate that the optimum parameters for the cross correlator are a modulation index of 0.67 combined with a normalized filter bandwidth BT of 0.408 for a smooth rolloff filter. In addition, we found that the receiver could tolerate input signal amplitude variations of up to 20% of the average value with only a 1-dB loss in performance. A comparison of theoretical and simulation results shows agreement of within 0.5 dB in E_b/N_o. The reasonably close agreement of theory and simulation provides a test on the validity of the simulation results. The effect of timing error on the receiver performance was also studied. Using a low-complexity asynchronous timing recovery algorithm, losses due to a timing error of 1 sample every 50 symbols were reduced to about 0.5 dB in E_b/N_o.

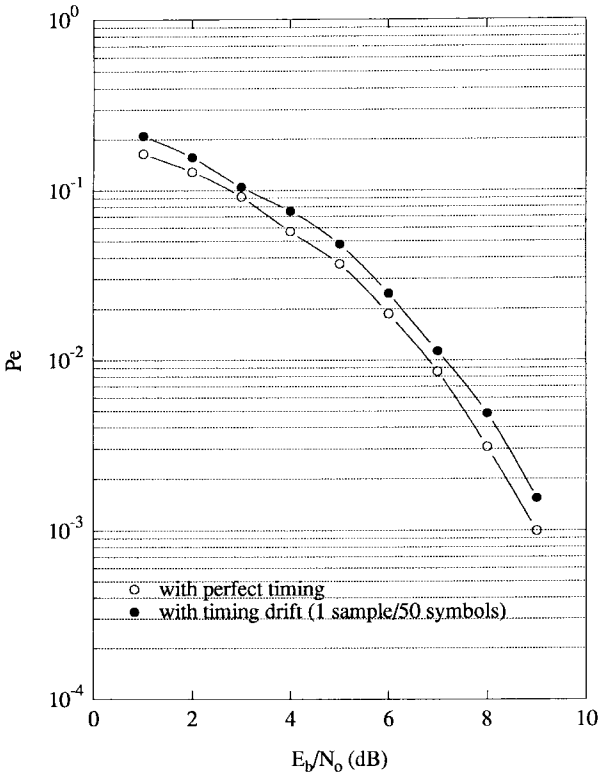

Fig. 9. Comparison of receiver performance with timing drift versus receiver performance with perfect timing assumed.

Acknowledgment

The authors thank Dr. L. Mason of the Communications Research Centre, Ottawa, Canada, for introducing them to the detector in [2].

References

[1] T. T. Tjhung and P. H. Wittke, "Carrier transmission of binary data in a restricted band," *IEEE Trans. Commun.*, vol. COM-18, pp. 295–304, Aug. 1970.
[2] J. H. Park Jr., "An FM detector for low S/N," *IEEE Trans. Commun.*, vol. COM-18, pp. 110–118, Apr. 1970.
[3] C. R. Cahn, "Improving frequency acquisition of a Costas loop," *IEEE Trans. Commun.*, vol. COM-25, pp. 1453–1459, Dec. 1977.
[4] F. M. Gardner, "Properties of frequency difference detectors," *IEEE Trans. Commun.*, vol. COM-33, pp. 131–138, Feb. 1985.
[5] F. D. Natali, "AFC tracking algorithms," *IEEE Trans. Commun.*, vol. COM-32, pp. 935–947, Aug. 1984.

[6] F. M. Gardner, "Demodulator reference recovery techniques suited for digital implementation," ESA Contract 6847/NL/DG, Final Rep., May 16, 1988.
[7] B. Koblents, "Asynchronous timing recovery in M-PSK data modems," Master's thesis, Queen's Univ., Kingston, Ont., Canada, 1992.
[8] H. R. Simpson, "Statistical properties of a class of pseudo-random sequences," *Proc. Inst. Elec. Eng.*, vol. 113, pp. 2075–2080, Dec. 1966.
[9] J. G. Proakis, *Digital Communications*, 2nd ed. New York, McGraw-Hill, 1989.
[10] F. Oberhettinger, *Tables of Fourier Transforms and Fourier Transforms of Distributions*. New York: Springer-Verlag, 1990.
[11] I. S. Gradshteyn and I. M. Ryshik, *Table of Integrals, Series, and Products*, corrected and enlarged ed. New York: Academic, 1980.
[12] K. A. Farrell, "Performance of the cross-correlator receiver for binary digital frequency modulation," Master's thesis, Queen's Univ., Kingston, Ont., Canada, 1993.

Kevin A. Farrell (S'92–M'95) received the B.Sc. degree in engineering physics in 1990, and the M.Sc. degree in electrical engineering in 1993, both from Queen's University in Kingston, Ont., Canada.

He worked in Barbados from 1993 to 1995 as a consultant and project manager in the areas of computer-based training courseware development and business process redesign. Mr. Farrell currently works as a consultant in Toronto, Ont., Canada for a company which develops, markets and implements Operations Support Systems for the telecommunications industry.

Peter J. McLane (S'68–M'69–SM'80–F'88) was born in Vancouver, BC, Canada, on July 6, 1941. He received the B.A.Sc. degree from the University of British Columbia, Vancouver, in 1965, the M.S.E.E. degree from the University of Pennsylvania, Philadelphia, in 1966, and the Ph.D. degree from the University of Toronto, Toronto, Ont., Canada, in 1969. He held a Ford Foundation Fellowship at the University of Pennsylvania and a National Research Council of Canada Scholarship at the University of Toronto.

From 1966 to 1967, he was a Junior Research Officer with the National Research Council, Ottawa, Ont. He joined the Department of Electrical Engineering, Queen's University, Kingston, Ont., in 1969 as Assistant Professor, and since 1977 he has held the rank of Professor. His research interests are in signal processing for digital communication systems. Usually, this involves computer-aided analysis, but lately he has been performing experimental work involving DSP implementation. He is a former research Trust Leader in Mobile and Satellite Systems for the Telecommunications Research Institute of Ontario (TRIO) and formerly a Major Project Leader in Mobile and Personal Communications for the Canadian Institute of Telecommunications Research (CITR). He is a joint author of *Introduction to Trellis-Coded Modulation with Applications* (Macmillan, 1991).

Dr. McLane is the chair of the IEEE Communications Society Communication Theory committee. He is a former Associate Editor for the *IEEE Communications Magazine* and former Editor of the IEEE TRANSACTIONS ON COMMUNICATIONS. In addition, he was co-editor of issues in the IEEE JOURNAL ON SELECTED AREAS IN COMMUNICATIONS and the *IEEE Communications Magazine*. He is also a member of the Association of Professional Engineers of Ontario and is listed in *American Men and Women in Science*. In 1994, he was a joint recipient of the Stentor Telecommunications Research Award.